*Tikrit Journal of Pure Science 21 (3) 2016* *ISSN: 1813 – 1662 (Print)*
*E-ISSN: 2415 – 1726 (On Line)*

# Study structural, dielectric and ferroelectric properties of Pb ($Zr_{1-x}$ $Ti_x$)$O_3$ ceramics near the morphotropic phase boundary

**Abdulsamee Fawzi Abdul Aziz AL-Bayati**
*Natural Ressources Research Center , Tikrit University , Tikrit , Iraq*
abdulsamee_fawzi@yahoo.com

## Abstract
In the present work, Pb($Zr_{(1-x)}Ti_x$) ceramics (x = 0.50, 0.48, 0.45 and 0.42) were prepared using the solid state reaction method, at the sintaring temperature (1100 $^oC$ ) for (6hr).X-ray diffraction results demonstrate that all the samples lie within the morphtropic phase boundary (MPB) region in the pure perovskite tetragonal structure with Miller transactions (100), (110), (111), (200), (210), (211), (220), (103) and (311) that the prevailing trend is (110) and the results of plasticity microwave very close sense of distance intra-convergent also relatively few crystalline defects. Increasing the bulk density of the true density of altered concentration of zirconium and titanium. Results of the examination microscope also showed that the particle size ($D_{nm}$) be tight between the samples and the homogeneity of the granules, as well as increasing the homogeneity of compositional structure, causing an improvement in the structural and electrical properties. Shown technique results EDAX compound of the interacting elements of the composition and there is little difference between the real weight and the weight is noticeable. The temperature and concentration of titanium dependences of the dielectric constant of the ceramics has been investigated in detail. Excellent dielectric properties have been obtained for the selected compositions. Polarization-Elctric field hysteresis studies were carried out for all compositions at room temperature. It was found that with the increase of concentration of titanium content in the composition the remnant polarization decreases and ferroelectric loops get constricted.

**Keywords:** X-Ray Diffraction; perovskite; Morphtropic phase Boundary; Ferroelectric hysteries.

## 1. Introduction
Ferroelectric materials show a number of desirable properties such as a Switchable polarization, high piezoelectric responses and high dielectric constants. For this reason, they are widely used in devices such as memory elements, ultrasound generators, capacitors, gas igniters and many more [1]. One of the rare examples of aferroelectric material is Lead Zirconate Titanate (Pb($Zr_{x-1}Ti_x$)$O_3$), which has been studied extensively over the past decade as it is one of the most promising ferroelectric materials with high Curie temperature (Tc) [2]. The PZT offers a wide range of properties that make them very attractive candidates for a variety of microelectronic and sensing applications. For the past few decades, the solid solution $PbZrO_3$-$PbTiO_3$, commonly known as PZT, has dominated commercially because of its superior dielectric and piezoelectric properties. In particular, its large piezoelectric response has made PZT one of the most widely used materials for electromechanical applications [3].
The aim of the present work was to prepare the lead zirconate titanatePb($Zr_{1-x}Ti_x$) (PZT) ceramics where 0.50, 0.48, 0.45 and 0.42, named as PZT-I, PZT-II, PZT-III and PZT-IV by solid state reaction method and to determine their structural and electrical properties. In this work, the prepared samples were characterized by X-ray diffraction (XRD) (model Bruker D8 Advance), and scanning electron microscope (SEM) (JEOL Analytical Scanning Electron Microscopy Model JSM-6360a). Ferroelectric loop tracer (Radiant Technologies) was used to investigate the structural analysis, surface morphotogical and electrical properties of the PZT ceramics.

## 2. Experimental
Pb ($Zr_{1-x}Ti_x$)$O_3$ samples (designated as PZT-I (x = 0.50), PZT-II (x = 0.48), PZT-III (x = 0.45) and PZT-IV (x=0.42) have been synthesized using solid state reaction technique. The powders of PbO (99.9%), $ZrO_2$ (99.9%) and $TiO_2$ (99.9%) were used as raw materials. Required amount of powders were mixed thoroughly milled in agate mortar and calcined at 800 $^oC$ for 4 hrs. The calcined powders were milled for 3 hours, and then pressed into pellets of diameter 10 mm and 2-3 mm in thickness. The samples in the form of pellets were sintered at 1100 $^oC$ on the sample bamied in the same powder in closed crucible for 12 hrs. The flow chart of preparation is shown in Fig. 1.

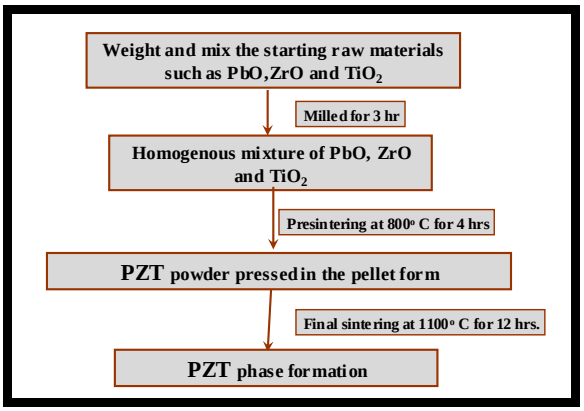


**Fig. 1. Flow chart for synthesis of Pb ($Zr_{1-x}Ti_x$)$O_3$ samples**

The x-ray diffraction patterns of all the samples were recorded using x-ray diffactometer (model Bruker D8 Advance), with CuKα radiations (λ=1.5418 Å) at a scanning rate of 0.4 sec/step. The lattice parameters

(a and c) and Miller indices (hkl) for tetragonal structure are related by [4].

$$\frac{1}{d^2}=\frac{(h^2+k^2)}{a^2}+\frac{l^2}{c^2} \quad \ldots\ldots (1)$$

The average particle size ($D_p$) of the samples is calculated using Scherrer's equation [6].

$$D_p=\frac{k\lambda}{\beta\cos\theta} \quad \text{----- (2)}$$

Where k = 0.89 (assuming the particles are spherical in shape); λ = wavelength of X-ray wavelength; β = full width at half maximum (FWHM) of the diffraction peak; and θ = angle of diffraction.

The X-ray density of the ferroelectric was calculated using the formula [7-8],

$$\rho_2=\frac{M}{N_A a^2 c} \quad \text{-------- (3)}$$

Where, M is molecular weight expressed in grams, 'a 'and 'c' are lattice constants and N is Avogadro's number (6.023 x $10^{23}$ molecule / mole).

The actual density of the samples can be Hendrick and Adams method [9].The method depends upon the weight of the sample in air and weight in a liquid of known density in which the sample is insoluble. In the present studies xylene was used as liquid in which ferrite/ ferroelectric/ composite sample were immersed. For these samples xylenes ( $\rho$ =0.861 g/cm$^3$ at 20$^0$C) was used. The actual density ( $\rho_a$ ) was calculated using the formula [9].

$$\rho_a=\frac{Weight\ of\ sample\ in\ air}{Weight\ of\ sample\ in\ air-Weight\ in\ xylene}\times density\ of\ xylene \quad \text{----- (4)}$$

$$\rho_a=\frac{W_{air}}{W_{air}-W_{Liquid}}\times\rho_{Xylene}$$

The porosity was calculated from the relation [10].

$$\text{Porosity}=\left\{\frac{100\,(\rho-\rho_a)}{\rho_x}\right\}\% \ldots. (5)$$

Scanning Electron Microscope (JEOL, Analytical Scanning Electron Microscopy Model JSM – 6360A) was used to obtain the microstructure and elemental analysis of the composites. Average grain size (grain diameter) of the sample was determined from SEM micrographs by linear-intercept technique [11].

The dielectric measurements were carried out in the wide range of frequency measurements viz. 100 Hz to 5 MHz at room temperature and at four fixed frequencies viz. 1 kHz, 10 kHz, 100 kHz and 1 MHz in the wide range of temperature measurements using LCR Meter Bridge (model HIOKI 3532-50 LCR Hi TESTER). The dielectric constant (έ) was calculated by using the formula [12].

$$\varepsilon'=\frac{C_P\times d}{\varepsilon_o A} \quad \text{--------- (6)}$$

where Cp is parallel plate capacitance in pico-farad, d is thickness of the pellet in cm, A is area of cross section of pellet = π r$^2$ (r is radius of the pellet in cm) and $\varepsilon_o$ is constant of permittivity of free space 8.85*10$^{-12}$ F/cm. The varation of dielectric constant and loss tangent with temperature was studied at four fixed frequencies viz. 1 kHz, 10 kHz, 100 kHz and 1 MHz, by recording the same parameters. Saturation polarization, remanence polarization and coercivity values were obtained using Automatic P-E hysteresis loop tracer system (Marine India Elect. Pvt. Ltd.) [13].

## 4. A. 3. Results and discussion

### 4. A. 3. 1 Structural property by XRD.

The X-ray diffraction pattern of ferroelectric samples having general formula $Pb(Zr_{1-x}Ti_x)O_3$ where( x = 0.42, 0.45, 0.48 and 0.50) are shown in Fig.2. All the patterns were indexed using JCPDS data for PZT ferroelectric card no. (10-325), which depict pure perovskite tetragonal structure of PZT samples. There are no extra peaks indicating purity of the samples synthesized. The positions of all the Bragg lines were used to obtain the interplaner spacing and these values were used to index the peaks. The observed and calculated'd' values are given in Table 1.These are in good agreement with each other for all indexed planes in case of all samples [14**].**

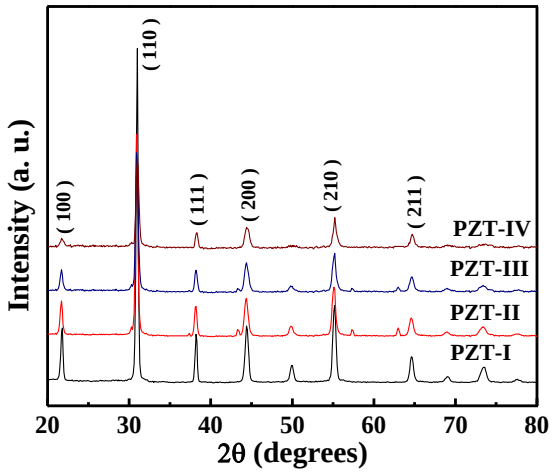


**Fig.2. X-ray diffraction patterns of PZT-I, PZT-II, PZT-III and PZT-IV samples**

**Table 1 Miller indices and inter planer spacing for PZT-I, PZT-II, PZT-III and PZT-IV samples.**

| (hkl) | $d_{std.}$ | PZT-I | PZT-II | PZT-III | PZT-IV |
|---|---|---|---|---|---|
| (100) | 4.08 | 4.11 | 4.10 | 4.09 | 4.05 |
| (110) | 2.87 | 2.88 | 2.87 | 2.87 | 2.86 |
| (111) | 2.35 | 2.35 | 2.34 | 2.33 | 2.33 |
| (200) | 2.04 | 2.05 | 2.04 | 2.01 | 2.03 |
| (210) | 1.82 | 1.84 | 1.83 | 1.81 | 1.81 |
| (211) | 1.66 | 1.67 | 1.69 | 1.70 | 1.66 |
| (220) | 1.43 | 1.44 | 1.47 | 1.48 | 1.43 |
| (221) | 1.29 | 1.31 | 1.33 | 1.36 | 1.30 |
| (310) | 1.22 | - | - | 1.21 | |

The graph of lattice parameter verses the function F(θ) (Nelson- Riley formula) [15] is given in Fig. 3, where,

$$F(\theta) = \tfrac{1}{2}\left[(\cos^2\theta/\sin\theta) + (\cos^2\theta)/\theta\right] \quad \text{----- (7)}$$

Straight line plots are obtained for all samples, extrapolating the lines to F (θ) = 0 at θ = 90° gives corrected value of lattice constant.

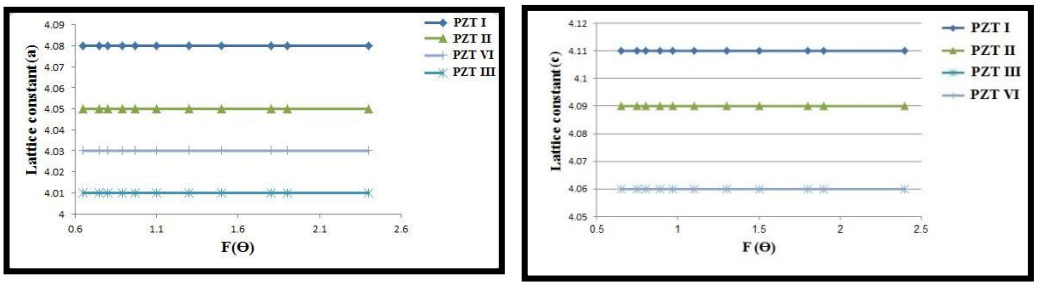


**Fig. 3. The lattice parameter (a,c) versus the function F(θ)**

The concentration dependence of the lattice parameters (a, c) with an accuracy of ± 0.02Å was determined form XRD data for all samples and given in Table 2. The tetragonality (c/a ratio) of the samples remains approximately same in all samples. This indicates that no structural change was observed even though the concentration of zirconium and titanium [16].

**Table 2 lattice parameter (a, c), ratio (c/a), FWHM, crystallite size (D), x-ray density ($\rho_x$), actual density ($\rho_a$) and porosity (p).**

| Samples | a ( A°) | c ( A°) | c / a | FWHM (degree) | crystallite size D (nm) | $\rho$ x-ray ($g/cm^3$) | $\rho$ actual ($g/cm^3$) | Porosity % |
|---|---|---|---|---|---|---|---|---|
| PZT I | 4.08 | 4.11 | 1.0073 | 0.228 | 0.6073 | 8.081 | 4.1122 | 49.11 |
| PZT II | 4.05 | 4.09 | 1.0098 | 0.203 | 0.6832 | 7.880 | 4.1375 | 47.49 |
| PZT III | 4.01 | 4.06 | 1.0124 | 0.223 | 0.6220 | 8.313 | 4.3649 | 47.49 |
| PZT IV | 4.03 | 4.06 | 1.0074 | 0.216 | 0.6412 | 8.264 | 4.5543 | 44.88 |

**3.2 Surface Morphological studies by SEM:**

SEM photographs of PZT-I, PZT-II, PZT-III and PZT-IV were shown in figure 4. Shape of the grain was not regular, large no of pores observed. Grain size measured for all samples 0.52, 0.51, 0.53 and 0.49 μm respectively.

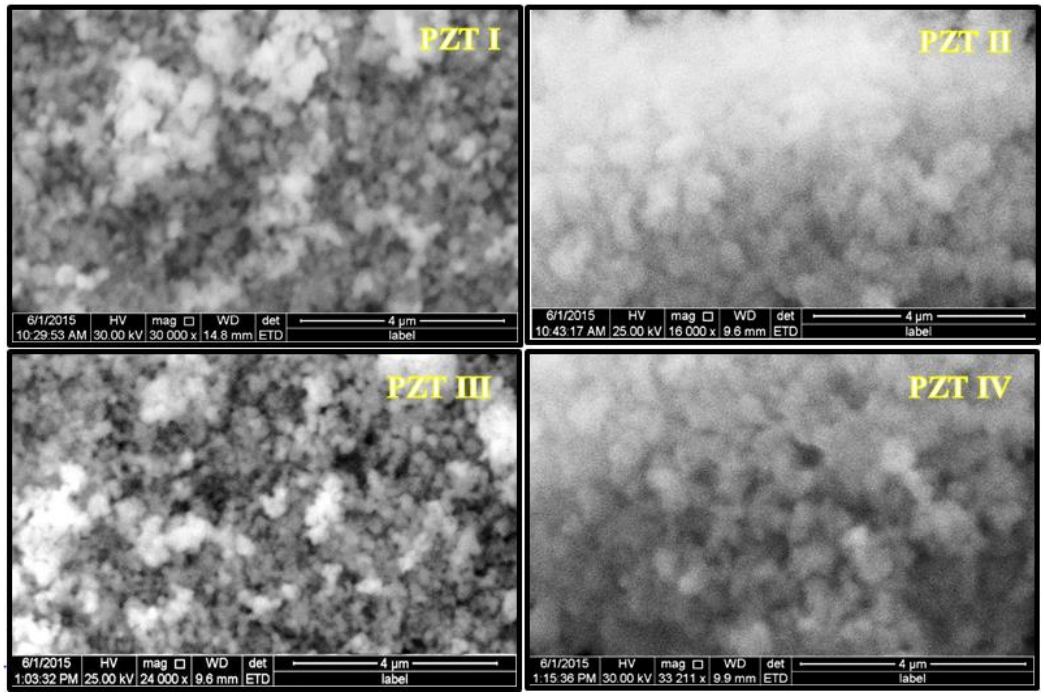


**Fig. 4. SEM micrograph of PZT-I, PZT-II, PZT-III and PZT-VI samples**

It is clear that ceramic samples of a size darling evenly matched, as was obtained graphs that distribution of elements for each installation samples show $Pb(Zr_{1-x}\ Ti_x)\ O_3$ at 1100 °C on the degree of heat and using EDAX technique as shown in Figure 5.

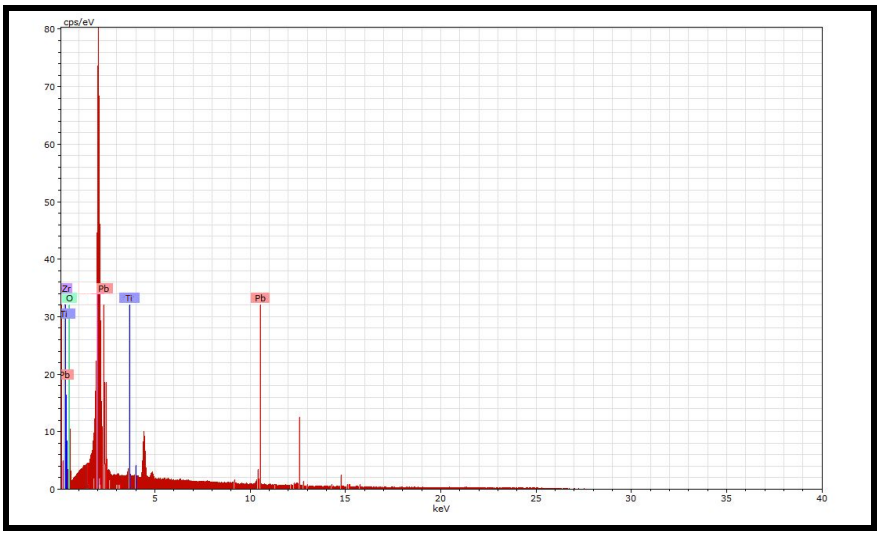


**Fig.5 distribution of elements that have been obtained from the microscope on using SEM EDAX technique to sample PZT-I.**

It was also obtained on the analysis of the elements involved in the installation sample ceramic Pb ($Zr_{1-x}$ $Ti_x$) $O_3$ using EDAX technique for example PZT-I as shown in the table (3), who confirmed the compound of the interacting elements formation It was noted that there is little difference between the expected weight and the weight is noticeable [17].

**Table. 3. The results obtained from the microscope on using the technique in the EDAX analysis of the elements of the PZT-I sample.**

| Element | Number | Series | Weight % | Atomic % | Error % |
|---|---|---|---|---|---|
| Pb | 82 | L- Series | 42.67 | 43.73 | 1.18 |
| Zr | 40 | L- Series | 31.39 | 44.63 | 1.69 |
| Ti | 22 | K- Series | 17.22 | 0.79 | 0.07 |
| O | 8 | K- Series | 8.70 | 10.85 | 0.04 |

### 3.3 Dielectric Properties

#### 1) Frequency dependent variation

The effect of frequency on dielectric constant (έ) at room temperature for all samples is illustrated in Fig. 6(a). From Fig. 6(a), it is clear that dielectric constant decreased with increasing frequency and finally at higher frequencies attains almost constant value for all the samples. This is obvious because of the fact that the species contributing to the polarizability are lagging behind the applied field at higher frequency [18]. The variation of dielectric constant with frequency reveals the dispersion due to Maxwell-Wagner [19] type interfacial polarization, which is agreement with Koop's phenomenological theory [20]. The large values of dielectric at lower frequency are mainly due to presence of all type of polarization i.e. $P_{total} = P_e + P_i + P_d + P_{sc}$ where subscripts indicate the electronic, ionic, dipolar and space charge contributions respectively. According to Sarah et al [21], the polarization in ferroelectric is through a mechanism similar to the conduction process. The exchange of electrons between ferrous ions ($Zr^{2+}$) and ferric ions ($Ti^{3+}$) on the octahedral site may lead to local displacement of electrons in the direction of applied field and these electrons determine the polarization. The polarization decreased with increasing frequency and then reaches a constant value due to the fact that beyond a certain frequency of external field the electron hopping cannot follow the alternating field. Fig. 6(b) shows the dielectric loss (tan δ) as a function of frequency at room temperature for all samples. It can be seen that the dielectric loss decreases with increasing frequency [22]. Fig. 6 ( c ) show the variation of imagunare part of dielectric constant with frequency for $Pb(Zr_{(1-x)}Ti_x)O_3$ composites. The imagunare part of dielectric constant variation show similar trend discussed for dielectric constant and dielectric loss. It can be seen that dielectric constant imagunare decrases with increase frequency. Similar explanation in case $(Ba_yPb_{1-y})(Zn_{1/3}Nb_{2/3})O_3$ ceramics is given by Byung-Young Ahn[23].

*ISSN: 1813 – 1662 (Print)*
*E-ISSN: 2415 – 1726 (On Line)*

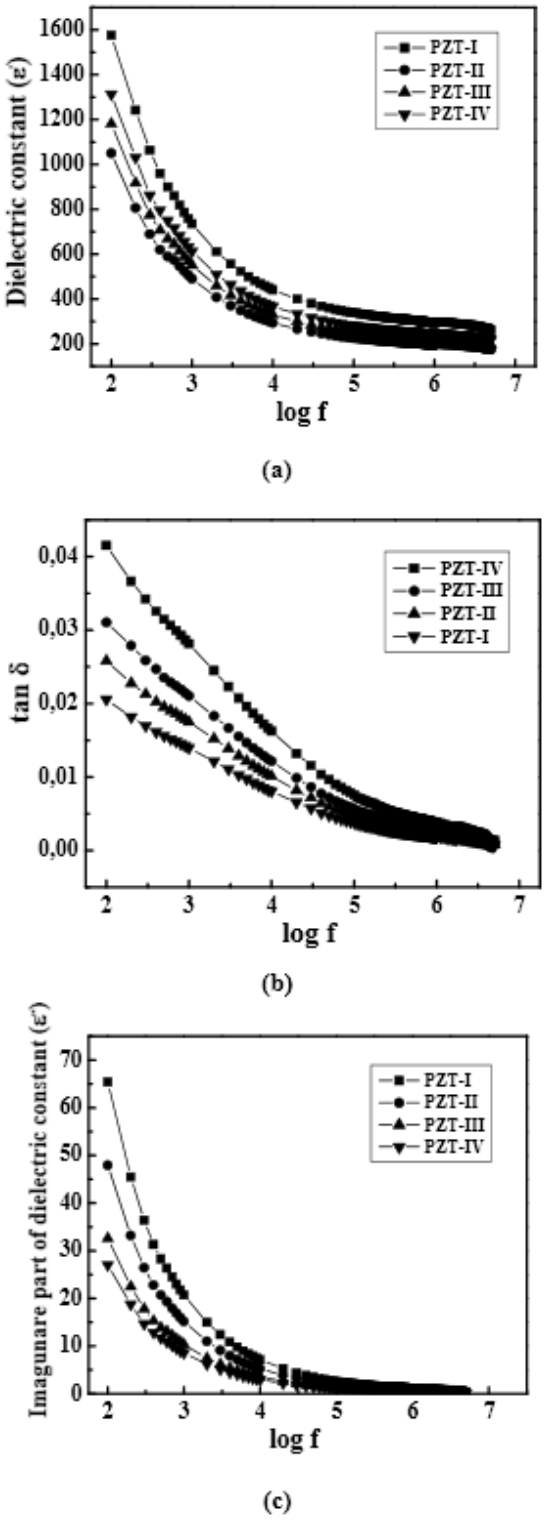


**Fig. 6 (a-c) Frequency dependent version of a) dielectric constant b) dielectric loss c) imagnare of dielectric constant for $Pb(Zr_{1-x}Ti_x)O_3$ composites.**

**2) Temperature dependent variation**

Fig. 7. (a-d) and Fig.8. (a-d) shows the dielectric constant (ε') and dielectric loss behavior as a function of temperature measured at 1 kHz, 10 kHz, and 100 kHz, and 1 MHz for PZT-I, PZT-II, PZT-III and PZT-IV composites respectively. The dielectric constant and dielectric loss increases with rise in the temperature up to transition of Curie temperature (Tc) and then decreases for all the samples. It also decreases with the increases frequency. Therefore, at low temperatures, the more charge carriers (binaries pole) may not itself directed towards the external electric field hanging and this is attracting shipment weak carriers and thus be low dielectric constant

*ISSN: 1813 – 1662 (Print)*
*E-ISSN: 2415 – 1726 (On Line)*

values, when temperatures rise, the charge carriers have the thermal energy necessary to be able to change with electric field easily hanging and when this case be well contribute to polarization and thus dielectric constant increases with increasing temperature. Until it reaches up to the transition temperature (degrees Curie temperature) (Tc) as the insulation of Barakherbaiah turns into Verokahrbaiah amounting to 425 $^{o}$C for PZT-I, 378 $^{o}$C for PZT-II, 317 $^{o}$C for PZT-III and 281 $^{o}$C for PZT-IV respectively, and at this temperature less polarization process and then dielectric constant begins to decreased with increasing temperature and frequency [24].

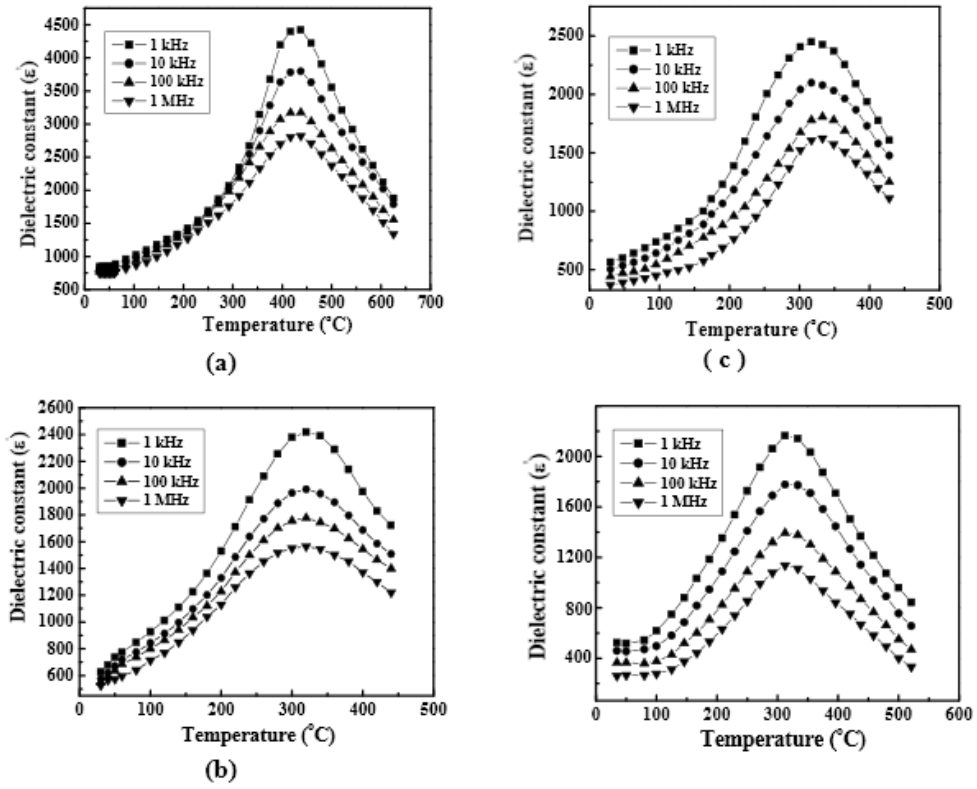


**Fig 7(a–c) Variation of dielectric constant with temperature for PZT-I, PZT-II, PZT-III and PZT-IV ferroelectric**

*ISSN: 1813 – 1662 (Print)*
*E-ISSN: 2415 – 1726 (On Line)*

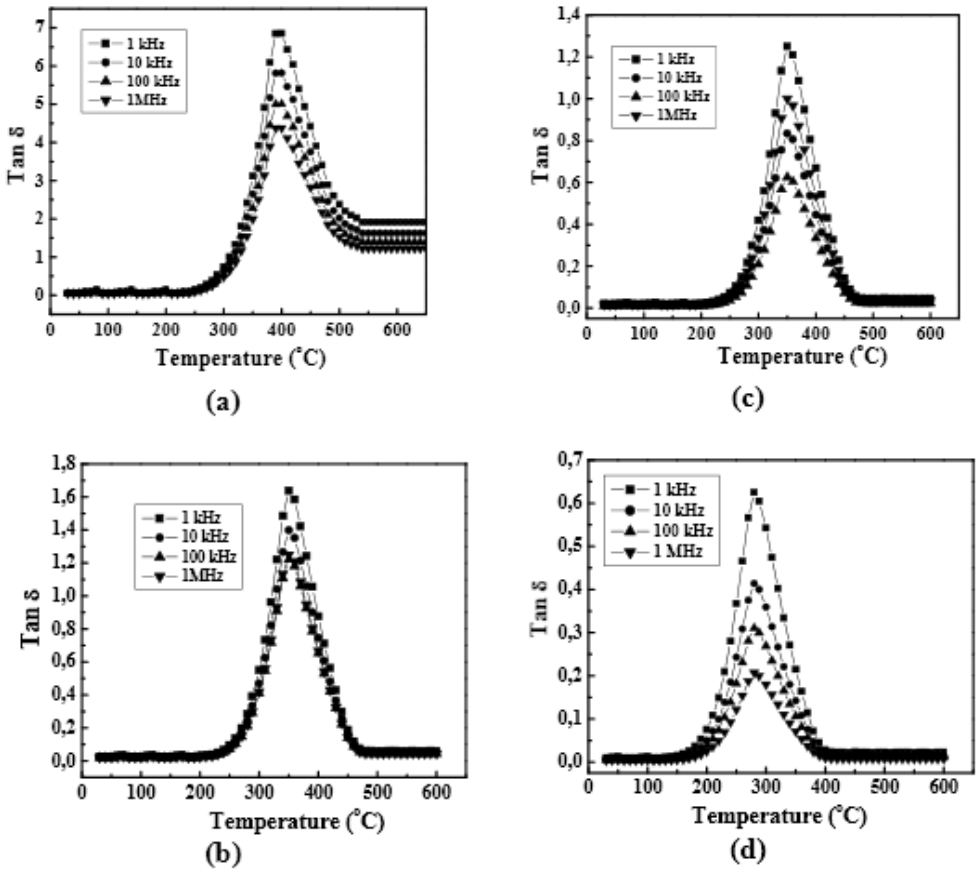


**Fig 8 (a-d) Variation of dielectric losses with temperature for PZT-I, PZT-II, PZT-III and PZT-IV ferroelectric**

The nature of the peak observed at transition temperature is broad. The degree of broadness also varies with composition and is measured in terms of diffusivity parameter γ. This diffusivity parameter or degree of broadness (disorder) is calculated using the expression [25]

$$\ln\left(1/\varepsilon - 1/\varepsilon_{max}'\right) = \gamma \ln\left(T - T_{max}\right) + a$$

where έ $_{max}$ is the maximum value of έ as observed at the transition temperature, ($T_c$) and γ the diffusivity parameter. The values of 'γ' lie between 1 and 2 for normal and diffused phase transition (DPT), respectively, which was extracted from the plot shown in Fig. 9 of ln (1/έ – 1/$έ_{max}$) with ln ( T-$T_{max}$) at 1 kHz for PZT-I, PZT-II, PZT-III and PZT-IV ceramics. Dots represent the experimental data and solid lines are the results of the linear fils. It is seen that for all the composites value of 'γ' greater than 1 indicating diffused phase transition. The values of 'γ' for PZT-I, PZT-II, PZT-III, and PZT-IV are 1.17, 1.41, 1.15 and 1.33 respectively, which are confirming DPT type behavior. Similar explanation in case $Pb(Zn_{1-x}Nb_x)O_3$ ceramics is given by A. V. Dixit [26].

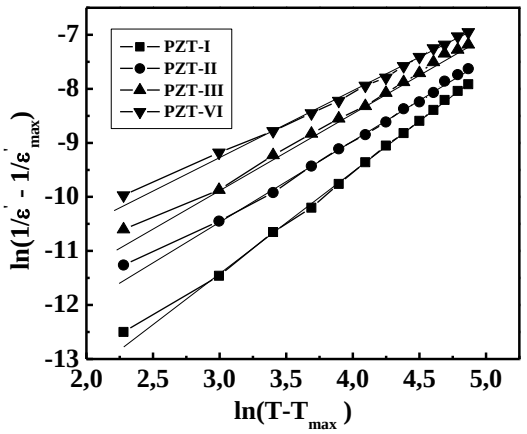


**Fig. 9 Dependence of ln (1/έ – 1/$έ_{max}$) with ln ( T-$T_{max}$) at 1 kHz for PZT-I, PZT-II, PZT-III and PZT-IV ceramics. Dots represent the experimental data and solid lines are the results of the linear fils**

### 3. 4 Ferroelectric properties

from the results of tests loop electrical Alhustrh (PE Loop) showed that the behavior of Alhustrh for Verokahrbaiah models compound Pb ($Zr_{1-x}$ $Ti_x$) $O_3$ record deviation solid state at fixed areas of interaction and at room temperature and are described in (Figure 10) was calculated Polarizing saturated (Ps) and polarization residual (Pr) and forced field (Ec) as shown in the table (4), as shown that bipolar

strongly depends on the hanging electric field, was also noted that the polarization reaches saturation and this is typical behavior of materials Elvirokahrbaiah [27], as the value of polarization remaining account (Pr) it found that, increasingly, the area forced (Ec) varies slightly as shown in Alhustrh ring, as between researchers Mohammed, Naik [28] that all of (Ps values) and (Pr) strongly depends on the particle size of the material and the value of the forced field (Ec), as between researchers Zhang, Zhao [29] are 9KV a less than the value obtained to in this research and that the coercive field (Ec) less mean size darling largest and vice versa and Baltaa should note the percentages used by Zhang, Zhao in composite study acceptable PZT This explains the decline b (Ec) and this is good compatibility with image SEM , that the high value of the residual polarization (Pr) means uniform distribution of the granules in all models, uniform distribution of the sites, a decrease crystal defects. It is important to note that the high value (Ec) is appropriate in most applications used in modern equipment and this means greater loss of power and boycotted the voltages and so to some extent this can be compensated if the samples Thoudy interaction solid-state manner [30].

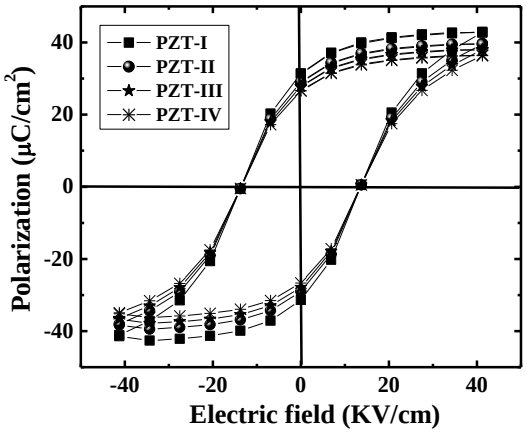


**Fig. 10 Polarization (P) versus electric field (E) curve for PZT-I, PZT-II, PZT-III and PZT-VI ceramic.**

**Table 4. The values of $E_c$, $P_s$, and $P_r$ obtained from the hysteresis loops of PZT-I, PZT-II, PZT-III and PZT-IV samples.**

| Samples | Remanent polarization $P_r$ (μC/cm$^2$) | saturation polarization $P_s$(μC/cm$^2$) | coercive fields $E_c$(V/cm) |
|---|---|---|---|
| PZT I | 147.862 | 202.9479 | 13.75 |
| PZT II | 230.3155 | 316.11945 | 13.78 |
| PZT III | 271.54225 | 372.70522 | 13.80 |
| PZT IV | 312.769 | 429.291 | 13.82 |

## 4. Conclusion

It has shown in the results of this research are many points of possible taking into account the practical applications and uses of the compound within minutes of work and preparation conditions and the most important of these conclusions that have been reached in this research:

1. The results of the examination of X-ray diffraction showed that the crystal structure of all the prepared models is four-installation as diffraction symmetry of the levels of peaks appeared (100), (110), (111), (200), (210), (211), (103), and (311) preferential direction(110).
2. Increase virtual density calculated from the results of X-ray diffraction (x-ray) resulting density of the cluster relative to the size of the samples of altered ratio of titanium, this leads to improved electrical properties.
3. The results of the formation factor calculation showed that the prevailing trend is (110) and there is no change in this direction for all samples.
4. Plasticity microwave account the outcome of a convergence of values for all samples shown this means that the distance is not much different interfaces and therefore crystal defects are relatively few.
5. Number of crystals varies with Ti, Zr.
6. Microscopic examination on the PZT ceramic composite results showed that the grains homogeneous and uniform particle size and evenly matched.
7. Technology showed the results of EDAX compound of stoichiometry composition and there is little difference in the real weight and the weight is noticeable.
8. Results of electrical tests showed a decrease in dielectric constant real values (ε ') and imagunare part of dielectric constant (ε ") as well as the dielectric loss (tanδ) very sharply with increasing frequency to some extent 3000KH and then be a gradual decrease with an increase in frequency, has It observed a gradual increase in the conductivity values alternating with an increase in frequency.
9. The results of change constant real insulation with temperature at different frequencies that the real insulation for all samples constant increases with temperature and frequency until it reaches the transition temperature (degrees Curie temperature) (Tc). Article shifting from developed Albarrakahrbaiah to phase Elvirokahrbaiah. The degree heat transformation of the samples are: 425 $^oC$ for PZT-I, 378 $^oC$ for PZT-II, 317 $^oC$ for PZT-III and 281 $^oC$ for PZT-IV respectively.
10. Results Alhustrh ring compound PZT shown that bipolar strongly depends on the hanging electric field and dipole increases with hanging area and thereby increase the polarization to be up to saturation as well as increasing polarization remaining area forced almost constant and thus the size of Habibi less.

## Acknowledgements

Author, A. F. Aziz wishes to thanks Tikrit University – Natural Ressources Research Center and the department of physics, university of pune - India for providing me the financial support during the course of my research. Iam thankful to the non-teaching staff of the department of physics, Mr. Valimble for their help and co-operation.

## References

[1] Damjanovic D, Science of Hysteresis ,ed. G Bertotti and I. Mayergoyz, Elsevier, 76 (1987) 241.
[2] B. Praveenkumar, H.H. Kumar , D.K. Kharat, B.S. Murty Materials Chemistry and Physics 112 (2008) 31–34
[3] Sweta Sharma, Md Soaib Khan, Rajiv Ranjan, B. Behera, R.N.P. Choudhary Volume III, Issue IX, September 2014 Ijltemas 2278 – 254
[4] D.meyer hofer, Transition to the ferroelectric state in barium titanate, physical review.112 (2011) 58.
[5] S.O. Pillai "Solid State Physics", New Age International Publishers Ltd., New Delhi (2002).
[6] C. Hammond," The Basic of Crystallography and Diffraction" Oxford University Press, Oxford (2001).
[7] C. Duran, S. T. McKinstry and G. L. Messing. J. Electroceram. 10 (2003) 47.
[8] A. M. Abdeen, O. M. Hemeda, E. E. Assem, M. M. El-Sehly., J. Magn. Magn. Mater. 238 (2002) 75.
[9] A. D. Sheikh and V. L. Mathe., J. Mater. Sci. 43 (2008) 2018.
[10] Xiwei Qi, Ji Zhou, Baorang Li, Yingchun Zhang, Zhenxing Yue, Zhilun Gui, and Longtu Li, J. Am. Ceram. Soc., 87 (2004) 1848.
[11] S. K. Kulkarni, "Nanotechnology: Principles and practices" (2007).
[12] L.S. Deshmukh, K. Krishnakumar, S. Balakrishna, A. Ramakrishna and G. Sasathaiah., Bull. Mater. Sci. 21 (1998) 219.
[13] Solymar and D. Walsh, "Lectures on the Electrical properties of Materials", Oxford University Press, Oxford (1984).
[14] T. Tunkasiri, Smart. Mater. Sci. 3 (1994) 243-247.
[15] S. A. Mazen, A. E. Abd El-Rahim, B. A. Sabrah, J. Mater. Sci. 22 (1987) 4177.
[16] K. K. Patankar, Ph. D. Thesis, Shivaji Univ., Kolhapur (2001)
[17] M. Prabu, Pb.D. Thesis, Pune Univ., Pune (2013).
[18] J. Paletto, G. Grange, R. Goutte and L. E.yraud, J. Phys. D: Apll. Phys. 7 (1974) 78-84.
[19] K. W. Wagner, Ann, Physik, 40 (1993) 818.
[20] C. G. Koops, Phys. Rev., 83 (1951) 121.
[21] P. Sarah and S. V. Suryanarayana, Indian J. Phys. 77 (2003) 449.
[22] Y.H. Tang, X.M. Chen, Y.J. Li, X.H. Zheng. Mater. Sci. Engg. B 116 (2005) 150.
[23] I. G. Austin and N. F. Mott Adv. Phys. 18 (1996) 411.
[24] Byung-Young Ahn and Nam-Kyoung Kim. J. Am. Ceram. Soc., 83 (2000) 1720-1726.
[25] V. L. Mathe, K. K. Patankar, U. V. Jadhav, A. N. Patil, S.D. Lotake, S.A. Patil, Ceramics, International. 27 (2001) 531.
[26] A. V. Dixit, Ph.D. Thesis, University of pune – pune- India (2003).
[27] A. R. James, B. S. Chandra Rao, S. V. Kamat, J. Subrahmanyam, K. Srinivas, O. P. Thakur., Smart. Mater. Struct. 17 (2008) 035020.
[28] M. S. Mohammed and R. Naik, J. Mater. Res. 11 (1996) 2588-2593.
[29] Q. M. Zhang and J. Zhao, IEEE Trans. Ultrason, Ferroelectr. Freq. Control. 46 (1999) 1518-1526.
[30] Pramod K Sharma, Z. Ounaies, V. V. Varadan and V. K. Varadan, Smart Mater. Struct. 10 (2001) 878-883.

*Tikrit Journal of Pure Science 21 (3) 2016* *ISSN: 1813 – 1662 (Print)*
*E-ISSN: 2415 – 1726 (On Line)*

# "دراسة الخواص التركيبية والعزلية والفيروكهربائية لسيراميك $Pb(Zr_{(1-x)}Ti_x)O_3$ بالقرب من الاطوار الحدودية"

**عبدالسميع فوزي عبدالعزيز البياتي**

*مركز بحوث الموارد الطبيعية ، جامعة تكريت ، تكريت ، العراق*

**الملخص**

تم تحضيرسيراميك تيتانات زركونات الرصاص ذات الصيغة الكيميائية $Pb(Zr_{1-x}\ Ti_x)O_3$ حيث أنّ $(x = 0.5,0.48,0.45,0.42)$ وذلك بإستخدام طريقة تفاعلات الحالة الصلبة حيث تم تلبيد النماذج المحضرة عند درجة حرارة $(1100^{\circ}C)$ ولمدة (12hr). حيث أظهرت نتائج حيود الاشعة السينية ان جميع النماذج الواقعة ضمن منطقة الاطوار الحدودية كانت ذات تراكيب بروفسكايت رباعية نقية ومعاملات ميلر (001), (100) , (110) , (111), (002) , (200) , (210) , (211) ,(220),(221), (103) وأن الإتجاه السائد هو(110) ونتائج المطاوعة الميكروية متقاربة جداً بمعنى المسافة البينية متقاربة أيضاً والتشوهات البلورية قليلة نسبياً. زيادة الكثافة الظاهرية عن الكثافة الحقيقية بإختلاف تركيز الزركونيوم والتيتانيوم. كما أظهرت نتائج فحص المجهر الألكتروني أنّ الحجم الحبيبي $(D_{nm})$ يكون متقارب بين النماذج وتجانس الحبيبات, بالاضافة الى ان زيادة تجانس البنية التركيبية قد سبب تحسننا في الخواص التركيبية والكهربائية. ان نتائج تقنية EDAX قد اظهرت تكوين المركب من العناصر المتفاعلة ، مع وجود اختلاف قليل بين الوزن الحقيقي والوزن الملاحظ . كما تم دراسة تاثير كل من درجة الحرارة وتركيز التتانيوم على ثابت العزل الكهربائي للمركبات السيراميكية بشكل مفصل. كما تم دراسة حلقات الهسترة الكهربائية ( P-E loop ) لجميع المركبات عند درجة حرارة الغرفة . أذ تبين ان زيادة تركيز نسبة التيتانيوم في المركبات الى تناقص مقدار الاستقطابية المتبقية والحصول حلقات محدودة.

**الكلمات الافتتاحية:** حيود الاشعة السينية، بيروفسكايت، الأطوار الحدودية، الهسترة الفيروكهربائية.